The effect of cell disruption on the extraction of oil and protein from concentrated microalgae slurries

Ronald Halim [a,b,c,d,*], Ioannis Papachristou [a], George Q. Chen [e], Huining Deng [f], Wolfgang Frey [a], Clemens Posten [b], Aude Silve [a]

[a] *Institute for Pulsed Power and Microwave Technology (IHM), Karlsruhe Institute of Technology (KIT), Eggenstein-Leopoldshafen 76344, Germany*
[b] *Institute of Process Engineering in Life Sciences, Bioprocess Engineering, Karlsruhe Institute of Technology (KIT), Karlsruhe 76131, Germany*
[c] *School of Biosystems and Food Engineering, University College Dublin, Belfield, Dublin 4, Ireland*
[d] *UCD Conway Institute, University College Dublin, Belfield, Dublin 4, Ireland*
[e] *Department of Chemical Engineering, The University of Melbourne, Victoria 3010, Australia*
[f] *School of Chemical Engineering and Technology, Hebei University of Technology, Tianjin 300130, PR China*

- Pre-treatments enhanced cell disruption in *Nannochloropsis* slurries.
- Neutral lipid yield was directly dependent on the degree of cell disruption.
- Mechanical disruption was more effective for neutral lipid recovery.
- Protein yield was determined by both cell disruption and linkage hydrolysis.
- Chemical disruption was able to extract both structural and soluble proteins.

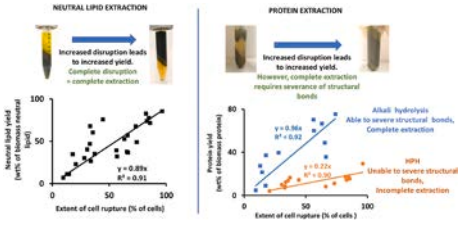

Keywords:
Microalgae
Wet biomass
Pre-treatment
Cell disruption
Lipid extraction
Protein extraction
Nannochloropsis

A B S T R A C T

Novel cell-disruption combinations (autolytic incubation and hypotonic osmotic shock combined with HPH or pH12) were used to investigate the fundamental mass transfer of lipids and proteins from *Nannochloropsis* slurries (140 mg biomass/g slurry).

Since neutral lipids exist as cytosolic globules, their mass transfer was directly dependent on disintegration of cell walls. Complete recovery was obtained with complete physical disruption. HPH combinations exerted more physical disruption and led to higher yields than pH12.

In contrast, proteins exist as both cytosolic water-soluble fractions and cell-wall/membrane structural fractions and have a complex extraction behaviour. Mass transfer of cytosolic proteins was dependent on cell-wall disintegration, while that of structural proteins was governed by cell-wall disintegration and severance of protein linkage from the wall/membrane. HPH combinations exerted only physical disruption and were limited to releasing soluble proteins. pH12 combinations hydrolysed chemical linkages in addition to exerting physical disruption, releasing both soluble and structural proteins.

* Corresponding author.
E-mail address: ronald.halim@ucd.ie (R. Halim).

1. Introduction

The high energy costs associated with large-scale biomass dehydration and mechanical cell disruption for the release of intracellular products remains a critical bottleneck in microalgae commercialisation (Halim, 2020; Halim et al., 2013; Vanthoor-Koopmans et al., 2013). Microalgal metabolites are intracellular in nature and can generally only recovered after liberation from cell-wall encapsulation (Halim et al., 2019b; Halim et al., 2020). The cell walls of many industrially promising microalgae genera (e.g., *Nannochloropsis* and *Chlorella*) are comprised of multilayered biopolymers that confer the cells with formidable defence against external processing (Baudelet et al., 2017; Canelli et al., 2021; Scholz et al., 2014). Finding an innovative means to weaken and/or rupture microalgae cell walls at scalable processing conditions (i.e., concentrated slurries with biomass concentration between 10 and 30 wt % of suspension instead of dried biomass or dilute culture with biomass concentration < 5 wt% of suspension) can aid product recovery, reduce the cost of biomass processing and increase biorefinery resource efficiency.

Nannochloropsis is an industrially attractive genus because of its high basal level of ω-3 fatty acid (up to 12 wt% of biomass), ability to aggressively accumulate biofuel-precursor neutral lipids (total lipid content up to 60 wt% of biomass under nutrient depletion) and proven metabolisms in assimilating wastewater nutrients (Menegol et al., 2019; Olmstead et al., 2013; Poddar et al., 2018; Russo et al., 2021; Shene et al., 2016). *Nannochloropsis* cells are highly resistant to cell rupture, possessing a rigid and structurally complex cell wall that comprises of an outer algaenan layer and an inner layer composed of cellulose and protein (Scholz et al., 2014).

Autolytic incubation and hypotonic osmotic shocks have previously been reported as novel preparatory steps to weaken *Nannochloropsis* slurries and enhance product recoveries (Halim et al., 2019a; Halim et al., 2019b; Halim et al., 2020; Halim et al., 2016). The two pre-treatments are unique compared to other reported methods as they were carried out at moderate operating conditions without the need of complex unit operations and relied mostly on cellular endogenous processes to catalyse cell-wall/membrane degradation. In the case of autolytic incubation (or thermally coupled dark anoxia incubation), *Nannochloropsis* slurries were incubated in darkness at 35-38℃ for 16 – 24 h (Halim et al., 2019a; Halim et al., 2016). This led to the activation of endogenous fermentation pathways which consumed structural sugars and thinned cell walls (by ca. 40%) (Halim et al., 2019a; Halim et al., 2019b). For hypotonic osmotic shock, *Nannochloropsis* slurries were subjected to multiple freshwater washing (and reconstitution) which delivered reverse osmotic gradients and progressively compromised the structural integrity of the cell membranes/walls (Halim et al., 2020). Since the pre-treatments were reported in separate studies, their relative efficiency to each other has never been directly compared. Equally importantly, the two treatments can potentially be combined to produce an innovative slurry processing technology for low-energy, self-lysing biorefinery fractionation. This potential combination warrants investigation.

Even though it is accepted that increased cell disruption leads to increased product yields, direct correlations between the degree of cell rupture and product extraction kinetics have rarely been demonstrated (Halim et al., 2016; Safi et al., 2020; Yap et al., 2014). Such correlations are critical to the parametric optimisation of cell disruption, cost of biorefinery operation and the prediction of product yields at commercial scale. Equally importantly, studies investigating microalgae product extraction have generally assumed that different intracellular products have the same extraction behaviours (i.e, increased disruption leads to higher yields). Cytosolic or non-structural products, however, can be expected to exercise different mass-transfer behaviours compared to structural products incorporated into organellar and cell-wall structures. Biofuel-convertible neutral lipids (or triglycerides), for example, are accumulated in *Nannochloropsis* cells as storage globules (Bongiovani et al., 2020; Hulatt et al., 2017; Jia et al., 2015; Law et al., 2018; Simionato et al., 2011; Yap et al., 2016). Given their non-structural nature, the mass transfer of neutral lipids will depend on the degree of their liberation from the cell-wall encapsulation and thus the extent of physical disruption of the cells (Sierra et al., 2017). On the other hand, proteins in the cells exist in both cytosolic forms (e.g. nucleic acids) and as integral components of the cell walls/membranes (e.g. glycoproteins) (Phusunti & Cheirsilp, 2020; Safi et al., 2017; Safi et al., 2013; Safi et al., 2014; Scherer et al., 2019; Soto-Sierra et al., 2018). This dual non-structural/structural nature will lead to a more complicated mass transfer behaviour which depend on both physical destruction of cell walls and severance of chemical linkages with cell structures to render accessibility. To the best of our knowledge, no study has yet to investigate the fundamental discrepancies between the mass transfer behaviours of cytosolic and structural intracellular products from disrupted biomass.

This study had dual objectives. The first objective was to investigate the feasibility of combining novel cell-wall weakening microalgae pre-treatments (autolytic incubation, hypotonic osmotic shock) with mechanical and chemical methods for the direct recovery of neutral lipids and proteins from concentrated slurries. To achieve this objective, *Nannochloropsis* slurries (140 mg ash-free dried biomass / g slurry) were subjected to different combinations of biomass pre-treatment (e.g. autolytic incubation, hypotonic osmotic shock, or both) with mechanical (high-pressure homogenisation) or chemical (pH 12) disruption. The performance of the biorefinery system was evaluated in terms disruption efficiency and product yields (neutral lipids and proteins). The second objective of the study was to investigate if there are any discrepancies between the mass transfer behaviours of cytosolic products (e.g. neutral lipids) and those of structural products (e.g. proteins). To achieve this objective, the values of cell disruption were correlated with their respective neutral lipids yields and protein yields across all combinations. This study is the first to simultaneously investigate the mathematical dependence of neutral lipid recovery and protein recovery from microalgae slurries on the level of cell-wall disruption.

2. Materials and methods

2.1. Strain, cultivation and harvest

N.gaditana strain (SAG 2.99) was acquired from the Culture Collection Centre at Georg-August-Universitat Gottingen (SAG, Germany). After inoculation into a modified 3f medium on synthetic seawater in a bubble-column photobioreactor with 25 L working volume, the culture was cultivated with permanent white illumination (daily step increase from 120 to 370 μmol m^{-2} s^{-1}) and continuous CO_2-enriched aeration (air flow rate of 0.15 vvm and a CO_2-to-air ratio of 1/100 v/v) for 18 days as previously described (Halim et al., 2020). Nitrogen in the medium was depleted on day 10 of cultivation. There was a total of 7 cultivation cycles for biological replicates. At the end of each cultivation cycle, the culture was harvested from the photobioreactor and concentrated using a centrifuge with a swinging-bucket rotor at 3,000 *g* and room temperature for 15 min. The resulting slurry had a biomass concentration of 139.6 ± 12.6 mg of ash-free dried biomass / g of slurry. Approximately 480 g of slurry was generated from each harvest cycle. This was sufficient to supply all of the biomass needed for the experiments in section 2.2.

2.2. Biomass pre-treatment, cell disruption, lipid extraction, protein extraction

The slurry from each harvest (referred to as harvested slurries) was subjected to a series of pre-treatment, cell disruption and lipid/protein extraction steps as shown in Fig. 1. The slurry was divided into four separate batches, each undergoing a different pre-treatment step to weaken cell-wall integrity: no pre-treatment, autolytic incubation,

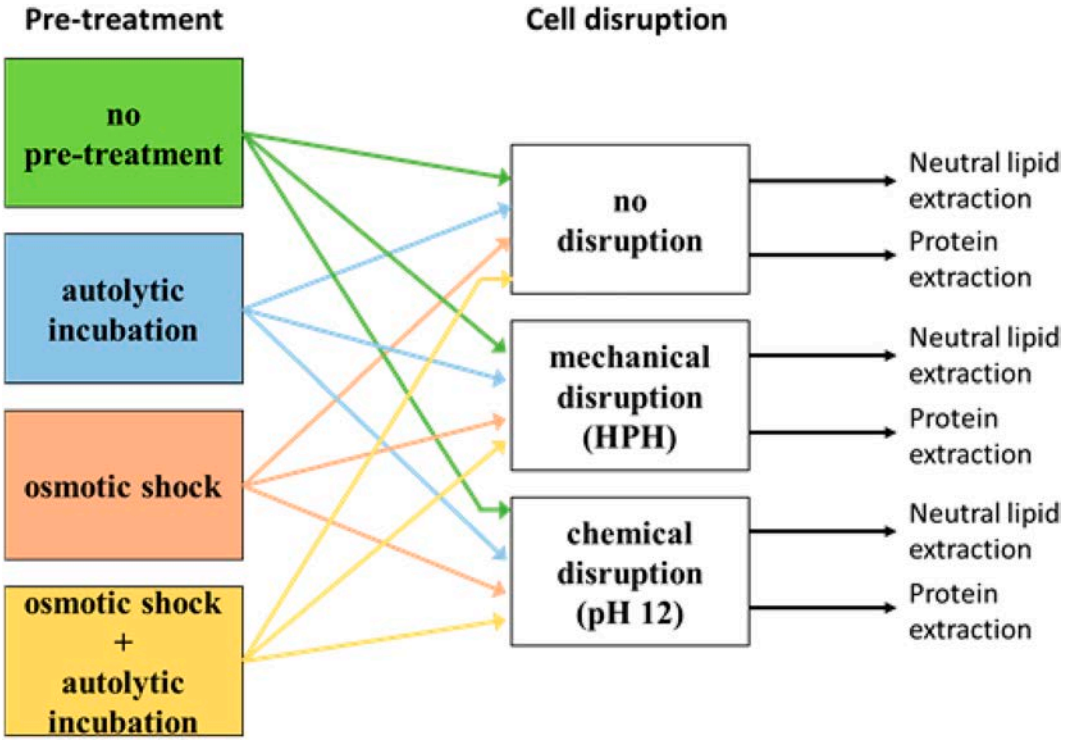

Fig. 1. Flow Diagram of the Experimental Matrix.

osmotic shock and a dual pre-treatment of osmotic shock followed by autolytic incubation. Details of the pre-treatment steps are presented in section 2.2.1 – 2.2.3. The pre-treated slurries were further divided into three batches, each subjected to no disruption, mechanical disruption (with high-pressure homogenisation), or chemical disruption with base (~pH 12). Details of the cell-disruption steps are given in section 2.2.4 – 2.2.5.

Table 1 shows the complete matrix of experiments carried out in the study. Overall, there were 12 different combinations of pre-treatment + cell disruption. The disrupted slurries were then subjected to either lipid extraction (with hexane) or protein extraction. Details of the lipid extraction and protein extraction steps are provided in section 2.2.6 and 2.2.7 respectively. For every harvest, microalgal slurry was harvested and immediately subjected to the combination of pre-treatment and disruption steps outlined in Table 1 immediately on the same day that it was harvested. Approximately 5 ml of each slurry (i.e., harvested slurries, pre-treated slurries and disrupted slurries) was collected between each step and stored at −20°C for analytical characterisation in section 2.3.

2.2.1. Autolytic incubation pre-treatment. Autolytic incubation was carried out by incubating the harvested slurry in darkness at 38°C for 16 h using a method modified from our previous studies (Halim et al., 2019a; Halim et al., 2019b). The slurry (~100 g) was placed in 2 × 50 ml vials leaving a small headspace for gas generation, covered in foil and stored in the oven at the required conditions.

2.2.2. Osmotic shock pre-treatment. Harvested slurry was subjected to hypotonic osmotic shock through two cycles of centrifugation and freshwater washing as previously described (Halim et al., 2020). In brief, 270 g of slurry was centrifuged (7500 *g*, 20°C, 10 min), supernatant decanted and weighed before DI water at a mass equal to the

Table 1
Experimental matrix showing the different combinations of pre-treatment and cell disruption steps. The extent of cell rupture, neutral lipid yield and protein yield of each experiment are provided.

Experiment no.	Pre-treatment step	Cell disruption step	Extent of cell rupture (% of cells in the harvested slurry)		Neutral lipid yield (wt% of total neutral lipid in the biomass)		Protein yield (wt% of total protein in the biomass)	
			mean	± std	mean	± std	mean	± std
1	no pre-treatment	none	0.0	0.0	7.9	8.5	1.5	2.0
2	no pre-treatment	mechanical disruption (HPH)	28.3	7.1	31.0	8.2	12.2	3.9
3	no pre-treatment	chemical disruption (pH 12)	13.4	5.6	4.0	5.7	6.7	2.4
4	autolytic incubation	none	10.3	8.4	5.1	1.2	9.8	3.1
5	autolytic incubation	mechanical disruption (HPH)	67.8	19.3	65.7	12.2	13.0	4.8
6	autolytic incubation	chemical disruption (pH 12)	65.8	0.7	30.2	16.7	38.8	9.1
7	osmotic shock	none	15.4	8.5	23.0	13.5	10.1	4.1
8	osmotic shock	mechanical disruption (HPH)	46.5	18.4	65.1	9.7	12.3	3.8
9	osmotic shock	chemical disruption (pH 12)	18.3	6.7	19.6	11.5	30.7	9.9
10	osmotic shock + autolytic incubation	none	32.4	13.9	25.9	19.7	23.4	10.2
11	osmotic shock + autolytic incubation	mechanical disruption (HPH)	86.8	6.5	77.8	6.6	17.4	5.7
12	osmotic shock + autolytic incubation	chemical disruption (pH 12)	62.5	8.3	41.1	10.7	66.2	8.6

collected supernatant (~143 g) was added to the microalgal pellet in order to reconstitute the slurry. The mixture was agitated, first with a spatula and then moderately with magnetic stirring for 30 min, to ensure complete homogeneity and the delivery of osmotic shock. Once the slurry was reconstituted, the hypotonic osmotic cycle was repeated a second time through another series of centrifugation, supernatant decanting, DI water addition and mixing.

2.2.3. Osmotic shock + autolytic incubation dual pre-treatment. Harvested slurry was subjected both osmotic shock and autolytic incubation. The slurry first underwent osmotic shock pre-treatment as described in section 2.2.2 before being incubated according to the autolytic incubation pre-treatment outlined in section 2.2.1.

2.2.4. Mechanical cell disruption with HPH. Pre-treated slurry (~40 g) was passed once through a high-pressure homogenisation (HPH) unit (Avestin EmulsiFlex-C3, Avestin, Canada) at 1000–1500 bar without any further dilution.

2.2.5. Chemical cell disruption with base (pH 12). Aqueous sodium hydroxide solution (1 M) was added dropwise to 25 g of pre-treated slurry to increase its pH value from 6.0 ± 0.3 to 12.3 ± 0.2. A total of 3 – 9 g of NaOH solution was added depending on the pre-treatment that the slurry had previously been subjected to. The mixture was moderately agitated before being incubated at 65℃ for 2 h.

2.2.6. Neutral lipid extraction. Lipid was extracted from disrupted slurry using two stages of biphasic hexane extraction. Hexane was selected for its strong affinity to neutral lipids, as demonstrated in our previous study (Halim et al., 2016). Disrupted slurry (4 g) was mixed with an equal mass of hexane, tumbled using a rotation wheel at room temperature (20℃) for 2 h and centrifuged to form four layers (7000 *g*, 20℃, 10 min). After carefully isolating the top hexane layer with a glass pipette, the remaining post-centrifugation layers were mixed using a spatula and the resulting mixture was further subjected to another hexane extraction stage. Hexane phases recovered from both extraction stages were pooled and dried under N_2 gas to enable gravimetric determination. The dried lipid extract was weighed before being re-dissolved in chloroform/methanol solution (2:1 v/v) and stored at −20℃ until further analysis.

2.2.7. Protein extraction. Protein was extracted from disrupted slurry by centrifugation (30000 *g*, 20℃, 10 min) and careful isolation of the resulting supernatant with a glass pipette. The supernatant was weighed and filtered (0.22 μm) to remove any residual biomass. After appropriate dilution with DI water to ensure that protein concentration falls within the linear range of the Lowry method, the supernatant was subjected to a modified Lowry analysis in accordance with the supplier's instructions. Protein concentration was measured against a 10-point linear bovine serum albumin (BSA) calibration curve and corrected for dilution factor.

2.3. Analytical characterisation

2.3.1. Biomass concentration and ash concentration of microalgal slurry. The dry material concentration of microalgal slurry was measured gravimetrically by drying a known amount of slurry on a pre-weighed aluminium cap at 60 °C in an oven for 16 h. Preliminary method development determined that 16 h of drying was sufficient to completely remove all waters from the slurries and obtain a constant final mass. At the end of the drying step, the cap was taken out of the oven and left to cool to room temperature for 10 min before being re-weighed.

The ash content of microalgal slurry was determined through a separate gravimetric measurement. A known amount of the slurry was dried on a pre-weighed porcelain crucible at 650℃ inside a high-temperature furnace for 16 h. At the end of the drying step, the crucible was taken out of the furnace and left to cool to room temperature for 10 min before being re-weighed.

The biomass concentration of microalgal slurry (139.6 ± 12.6 mg of ash-free dried biomass / g of slurry) was calculated by subtracting the dry material concentration of microalgal slurry with the ash content of the slurry.

2.3.2. Total lipid content of microalgal biomass. The total lipid content of microalgal biomass (harvested slurries and pre-treated slurries) was determined using a multiple-stage monophasic Bligh and Dyer extraction method as previously described (Halim et al., 2019b; Olmstead et al., 2013). Complete lipid recovery was verified through total bleaching of the cell debris after the final stage. The chloroform phases isolated from all extraction stages were pooled together, filtered (0.2 μm nylon syringe filter) and dried under N_2 gas for gravimetric measurement. The dried lipid was then re-dissolved in chloroform/methanol solution (2:1 v/v) for lipid fractionation and/or fatty acid methyl ester analysis.

2.3.3. Total protein content of microalgal biomass. The total protein content of microalgal biomass (harvested slurries and pre-treated slurries) was determined through high-temperature alkaline hydrolysis of the slurry to release all intracellular proteins and subsequent analysis of the isolated serum with a Lowry assay. Microalgal slurry (130 mg) was added to 2 ml of 1 N NaOH solution, heated at 95℃ for 1 h, cooled, and diluted appropriately with DI water to ensure that protein concentration falls within the linear range of the Lowry method. After centrifugation, the protein-rich serum was subjected to a modified Lowry analysis according to the supplier's instructions and the protein concentration was measured against a 10-point linear BSA calibration curve and corrected for dilution factor.

2.3.4. Total sugar content of microalgal biomass. The total sugar content of microalgal biomass (harvested slurries and pre-treated slurries) was determined using an anthrone-sulphuric acid assay. Microalgal slurry was diluted in DI water to a biomass concentration ranging between 0.1 and 0.4 g biomass /L. Freshly prepared starch standard solutions (Merck 1.01257, Merck, USA) in DI water were processed at the same time with microalgal slurries to generate a calibration curve. An aliquot of the diluted slurry or standard solution (400 μl) was mixed with 800 μl of freshly prepared anthrone reagent (0.1% w/v in 95% sulphuric acid) prior to being heated at 95℃ and 300 rpm for 16 min and transferred to ice for cooling. Absorbance of the solution was measured at 625 nm and the carbohydrate was calculated using the standard curve generated during the analysis and corrected for the appropriate dilution factor.

2.3.5. Lipid fractionation. Lipid solutions (e.g., neutral lipid extracts from hexane extraction in section 2.2.6 or total lipid extracts from Bligh & Dyer extraction in section 2.3.2) were separated into constituent fractions by sequential elution with different solvent systems (chloroform for neutral lipids, acetone/methanol 9:1 v/v for glycolipids and methanol for phospholipids) in a SampliQ pre-packed silica cartridge (Agilent Technologies, USA) as previously described (Halim et al., 2019b; Olmstead et al., 2013). Lipid fractions were dried under N_2 gas to enable gravimetric determination.

2.3.6. Fatty acid methyl ester (FAME) analysis. Lipid solutions (e.g., neutral lipid extracts from hexane extraction in section 2.2.6 or total lipid extracts from Bligh & Dyer extraction in section 2.3.2) were subjected to lipid transesterification and FAME analysis as previously described (Halim et al., 2019a). Chromatographic separation was carried out using an Agilent 7890B Gas Chromatography unit with a Flame Ionisation Detector (Agilent Technologies, USA) and a capillary column.

A known amount of C15:0 FAME internal standard was spiked to each solution to enable quantification (Sigma Aldrich, USA). Individual FAMEs were identified by retention-time comparison with a mixed FAME 18,917 Supelco standard (Sigma Aldrich, USA).

2.3.7. Cell disruption evaluation. In this study, the term 'cell disruption', 'cell rupture' and 'cell disintegration' are used interchangeably to denote the physical destruction of cells. The disruption efficiency of the pre-treatment (section 2.2.1 – 2.2.3) and cell disruption (section 2.2.4 – 2.2.5) steps was evaluated via automated cell count of the captured microscopic images. Harvested, pre-treated or disrupted slurry was diluted to an appropriate concentration for microscopic imaging (mass dilution ratio between 540 and 630x) and placed on a standard Neubauer haemocytometer (10 μl) for 15 min before being observed under a Zeiss Axioplan 2 light microscope (roughly 12 images of different 0.04 mm^2 haemocytometer grids were captured). The apparent number of intact cells in each captured image was evaluated using an automated ImageJ algorithm as previously described and corrected for dilution factor (Halim et al., 2019a). The extent of cell rupture (% of cells) for a specific slurry (e.g. pre-treated or disrupted slurry) measured the level of physical destruction of the cells and was calculated as follows:

$$\text{The extent of cell rupture} \quad \frac{\overline{C}_{\text{harvestedslurry}} - \overline{C}_{\text{specificslurry}}}{\overline{C}_{\text{harvested slurry}}} \hat{A} \cdot 100 \qquad (1)$$

where $\overline{C}_{\text{harvestedslurry}}$ was the average apparent number of intact cells for the harvested slurry (cells/g slurry) and $\overline{C}_{\text{specificslurry}}$ was the average apparent number of intact cells for the specific slurry (cells/g slurry).

2.3.8. Neutral lipid yield and protein yield calculations. The neutral lipid yield for an experiment was calculated as the ratio of the amount of neutral lipid extracted by hexane from the slurry (defined as the yield from section 2.2.6 followed by lipid fractionation in section 2.3.5 and measurement of dried lipid obtained in the chloroform fraction) to the total neutral lipid content of the biomass in the slurry (defined as the lipid obtained in section 2.3.4 followed by lipid fractionation in section 2.3.5 and measurement of dried lipid obtained in the chloroform fraction).

The protein yield of an experiment was calculated as the ratio of the amount of protein extracted from the slurry in section 2.2.7 to the total protein content of the biomass in the slurry (section 2.3.3).

3. Results and discussion

3.1. Biomass composition

The harvested *Nannochloropsis* biomass was rich in lipid, having a total lipid content of 607.0 ± 102.5 mg/g of ash-free dried biomass (with a total fatty acid content of 449.0 mg/g of ash-free dried biomass), total sugar content 249.9 ± 40.1 mg/g of ash-free dried biomass, and total protein content 143.1 ± 34.6 mg/g of ash-free dried biomass.

The biomass appeared to have suitable lipid-fraction and fatty-acid compositions for biofuel conversion, with neutral lipid fraction constituting the majority of total lipid (neutral lipid content 76.0 ± 16.1 wt % of total lipid or 461.4 ± 97.6 mg/g of ash-free dried biomass) and saturated (SFA) and monounsaturated (MUFA) fatty acids dominating the fatty acid profile of the total lipid (total SFA and MUFA contents 91.7 wt% of fatty acids or 411.8 mg/g of ash-free dried biomass). The fatty acids in the total lipid were comprised of the followings (in descending order): C16:0 (42.0 wt% of fatty acids), C16:1 (35.2 wt% of fatty acids), C18:1 (10.2 wt% of fatty acids), C20:5 (ω-3) (5.6 wt% of fatty acids), C14:0 (2.7 wt% of fatty acids), C20:3 (ω-6) (2.7 wt% of fatty acids) and C18:0 (1.5 wt% of fatty acids).

Neutral lipid is the preferred fraction for biofuel application given the potential toxicity of polar lipid head groups to transesterification catalyst (Halim et al., 2012; Olmstead et al., 2013). High levels of SFAs and MUFAs are also desirable as they form biodiesel with better cold-flow properties and higher oxidative stability (Halim et al., 2012; Olmstead et al., 2013). The alignment between lipid fraction and fatty acid suitability for biofuel production was expected as N-depleted *Nannochloropsis* biomass has previously been shown to accumulate neutral lipids (in the form of TAGs) constituting primarily of SFAs and MUFAs (Bongiovani et al., 2020; Jia et al., 2015; Olmstead et al., 2013; Simionato et al., 2013).

3.2. Effect of pre-treatment on cell disruption

Fig. 2a and Table 1 showed that the pre-treatment steps generally had a positive effect on the extent of *Nannochloropsis* cell rupture by both mechanical and chemical cell disruptions steps. Without the pre-treatment steps, HPH disruption and pH12 disruption were relatively ineffective in disrupting cells, being able to only rupture a mere 28 and 13% of available cells respectively. These findings further underscored the toughness of lipid-rich *Nannochloropsis* cell walls and the need for using a preparatory or pre-treatment step to weaken cell wall integrity and enhance the performance of subsequent cell disruption process for maximum product liberation. Theoretically, the disruption performance of either HPH and pH12 can be increased by subjecting the slurries to more severe process conditions (e.g. higher pressure and more passes for HPH or higher temperature and higher pH for alkali treatment), but this also leads to increased cost/energy requirements, degradation probabilities of labile components and undesirable hydrolytic side reactions.

The autolytic incubation was able to enhance cell disruption of HPH and pH12 by 2.4 folds and 4.9 folds respectively. As described in our previous studies (Halim et al., 2019a; Halim et al., 2019b), the increase in disruption efficiency was derived from cell-wall thinning which weakened cellular integrity and rendered the biomass more susceptible to subsequent processing.

Hypotonic osmotic shock was also found to be able to enhance cell disruption, increasing the extent of cell rupture of HPH and pH12 by 1.6 folds and 1.4 folds respectively. Compared to autolytic incubation, however, the weakening effect of hypotonic osmotic shock was less pronounced. This could be attributed to the fact that osmotic shock weakened biomass by increasing membrane permeability rather than directly thinning cell walls (Halim et al., 2020).

For HPH, the combination of the two pre-treatment steps (autolytic incubation and hypotonic osmotic shock) produced a synergistic effect which disrupted close to 90% of available cells. Overall, these findings suggested the effectiveness of the pre-treatment steps in enhancing *Nannochloropsis* cell disruption when applied either as an individual step or in combination with each other.

In industrial settings, it is important to note that the inclusion of a pre-treatment step would lead to increased cost and energy requirements for biomass processing. These extra costs should be balanced against the benefits of implementing such pre-treatment steps in terms of product yields. Our previous study showed that implementing the hypotonic osmotic shock in industrial scale (processing one tonne of slurry) accounted for<6% of the overall energy expenditure of biomass processing and led to a positive overall net energy balance of biomass processing for oleaginous microalgae with a neutral lipid content of more than 30 wt% biomass, such as the *Nannochloropsis* biomass used in this study (Halim et al., 2020). A comprehensive cost-benefit and energy assessment for the pre-treatment steps reported in this study, however, is beyond its scope. Instead, this study will use the microalgae biorefinery system to achieve multiple levels of cell disruption for thickly walled *Nannochloropsis* biomass for investigation into the fundamental mass-transfer behaviours of lipids and proteins.

3.3. Partitioning behaviour of mechanical and chemical cell disruption

In this section, the partitioning behaviour of the different slurries

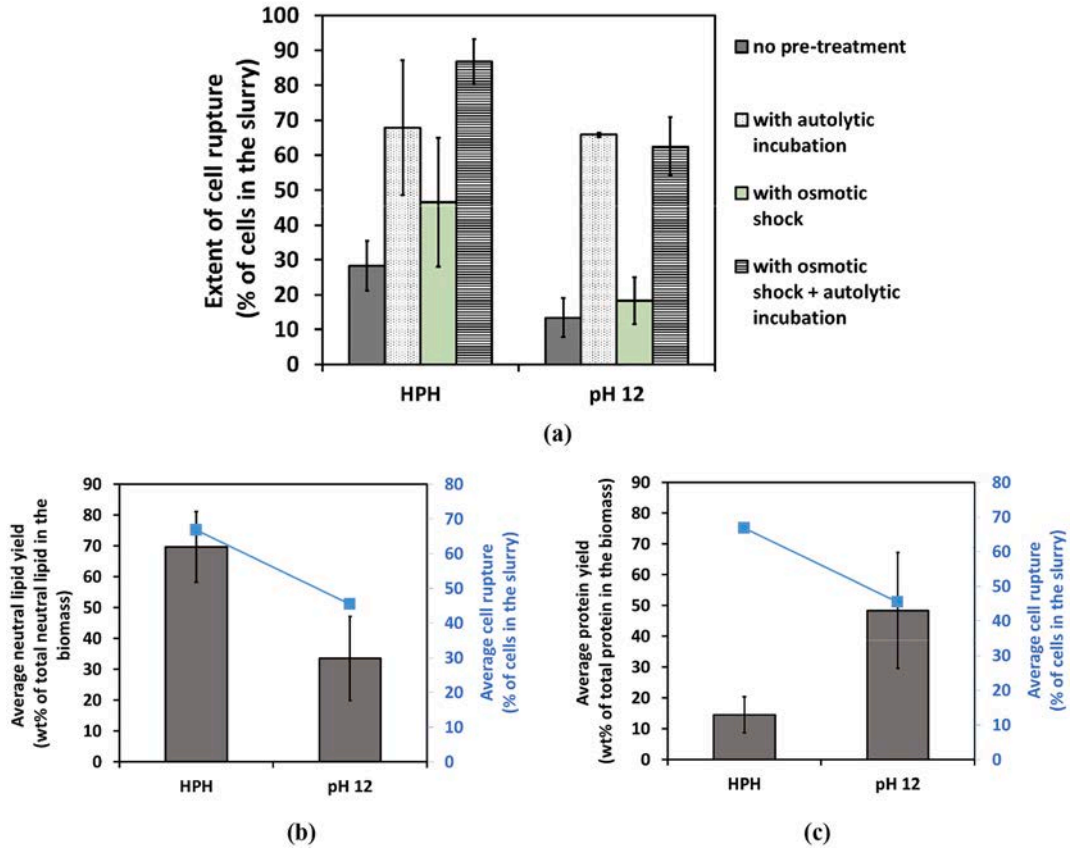

Fig. 2. (a) The effect of pre-treatment on the disruption performance of mechanical disruption (HPH) and chemical disruption (pH 12). (b) The effect of cell rupture on the neutral lipid yield obtained from mechanically disrupted (HPH) and chemically disrupted (pH 12) biomass. The average values of cell rupture and neutral lipid yield were calculated across experiments involving HPH (experiments 5, 8, 11 in Table 1) or pH 12 (experiments 6, 9, 12 in Table 1) (c) The effect of cell rupture on the protein yield obtained from mechanically disrupted (HPH) and chemically disrupted (pH 12) biomass. The average values of cell rupture and protein yield were calculated across experiments involving HPH (experiments 5, 8, 11 in Table 1) or pH 12 (experiments 6, 9, 12 in Table 1).

generated by the mechanical (HPH) and chemical (pH12) biorefineries was examined. As illustrated in Fig. 1, the disrupted *Nannochloropsis* slurries (post HPH or pH12 treatment) were subjected to both neutral lipid extraction (with hexane) and protein extraction. Once the extraction mixture was centrifuged, the desired products can be recovered from the appropriate phases.

Fig. 3 shows the phase partitioning of the four representative key scenarios encountered in our experimental matrix: 1) HPH + neutral lipid extraction with hexane (exp 11), 2) pH12 + neutral lipid extraction with hexane (exp 12), 3) HPH + protein extraction (exp 11), and 4) pH12 + protein extraction (exp 12). No discernible differences in the partitioning behaviour of biorefineries obtained from differently pre-treated biomass were noted, i.e. untreated slurries (exp 2), autolytically incubated slurries (exp 5), osmotically shocked slurries (exp 8) and both autolytically incubated and osmotically shocked slurries (exp 11) all shared the same partitioning behaviour once subjected to HPH and neutral lipid extraction with hexane. As discussed below, however, since pre-treated slurries are likely to experience more prolific cell disruption and product liberation, they produced darker layers with higher levels of dissolved products.

For HPH + neutral lipid extraction, the slurries partitioned into four distinct layers (Fig. 3a): 1) a top hexane layer containing the extracted lipids (which included neutral lipids and non-polar pigments, such as chlorophyll), 2) an emulsion layer comprised of a mixture of cell debris/intact cells, water and residual hexane, 3) an aqueous layer containing salts, and 4) a bottom cell debris layer containing water and cell debris. Readers are referred to our previous study for detailed understanding of the HPH + hexane extraction layers (Halim et al., 2016). Neutral lipids were gravimetrically quantified from the hexane phase.

For pH12 + neutral lipid extraction, the slurries partitioned into five layers (Fig. 3b): 1) a top hexane layer containing the extracted lipids, 2) a saponification layer where part of the extracted lipids appeared to have reacted with NaOH to form a gel-like soap layer, 3) an emulsion layer comprised of a mixture of cell debris/intact cells, water and residual hexane, 4) an aqueous layer containing salts and water-soluble pigment breakdown products, and 5) a bottom cell debris layer containing water and cell debris. The primary difference between HPH-lipid extraction layers and pH12-lipid extraction layers lies on the location of the recovered pigments. Unlike HPH layers where the extracted pigments remained water insoluble and thus partitioned in the hexane phase together with extracted lipids (thus contributing to the dark coloration of the lipid layer), the pigments in the pH12 biorefinery have reacted with NaOH to form water-soluble chlorophyllin which partitioned in the aqueous phase, contributing to the dark coloration of the aqueous layer and a lighter hexane phase (Li et al., 2016). The use of NaOH as a bleaching agent to remove chlorophyll from microalgae biomass/oil has previously been reported (Li et al., 2016).

Both HPH + protein extraction slurries (Fig. 3c) and pH12 + protein extraction slurries (Fig. 3d) separated into three layers: a top emulsion layer comprised of cell debris in water, a middle supernatant aqueous layer (or mid-natant layer) consisting of the released proteins, a bottom cell debris layer containing the intact cells, cell debris and dissolved salts in water. The extracted protein was quantified from the middle supernatant layer using a Lowry method.

3.4. Relationship between cell disruption and neutral lipid recovery

HPH combinations were generally found to be more effective in

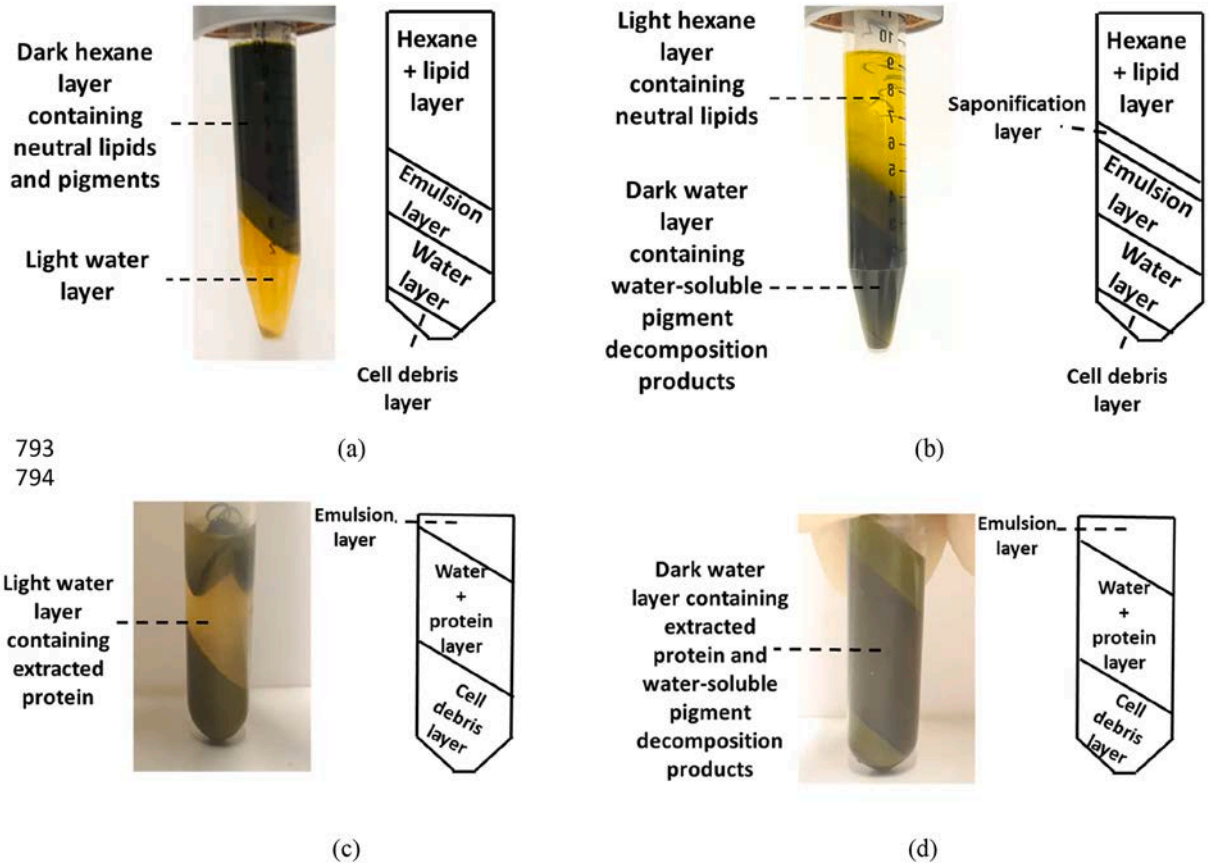

793
794

Fig. 3. Representative layer partitioning of post-centrifuged neutral-lipid and protein extraction slurries (a) Neutral-lipid extraction layers for HPH (experiment 11), (b) Neutral lipid extraction layers for pH 12 (experiment 12), (c) Protein extraction layers for HPH (experiment 11), (d) Protein extraction layers for pH 12 (experiment 12).

physically disintegrating cells compared to pH12 combinations (Fig. 2b). This was expected given the high level of shear force delivered by HPH disruption (Lee et al., 2017; Safi et al., 2017; Safi et al., 2014). Neutral lipid yield of the subsequent hexane extraction step appeared to follow the same pattern as cell rupture, with HPH combinations obtaining a higher yield compared to pH12 combinations and being the preferred disruption options for lipid recovery. These findings suggested a positive connection between cell rupture and neutral lipid yield.

To further probe the relationship between the extent of cell rupture and neutral lipid recovery, neutral lipid yield was plotted as a function of cell rupture across all experiments which included either mechanical or chemical disruption (Fig. 4a). The correlation revealed a linear relationship between the two variables (r^2 0.91). Equally importantly, with a gradient close to 1 (k 0.89), the correlation established that almost all of the available neutral lipids in the biomass can be recovered (e.g. neutral lipid yield 90 wt% of total neutral lipid in the biomass) if complete cell disruption had been achieved (e.g. extent of cell rupture 100% of cells in the slurry).

The direct dependence of neutral lipid recovery on the extent of cell rupture can likely be attributed to the nature of neutral lipids as cytosolic globules that are 'trapped' within the cell walls but are not chemically linked to any cellular structures or organelles (Bongiovani et al., 2020; Law et al., 2018; Simionato et al., 2013; Yap et al., 2016; Yap et al., 2014). The mass transfer of neutral lipids from the biomass into the extracting solvent was hence almost entirely dependent on the extent of their liberation from cell-wall encapsulation. Once these barriers were physically destroyed, the 'freed' neutral lipid globules became accessible to the extracting solvent for solubilisation. An increase in the degree of cell disruption therefore led to an increase in the amount of liberated neutral lipids which subsequently increased their mass transfer to the extracting solvent.

An interesting element of the relationship between cell disruption and neutral lipid recovery was its independence from disruption mode. The correlation depicted in Fig. 4a spanned both mechanically and chemically disrupted biomass, producing a single equation for both disruption modes. The correlation appeared to be accurate regardless of whether cell-wall breakage was achieved via a mechanical means or a chemical means. Such independence from cell disruption mode was again likely ascribed to the non-structural nature of neutral lipids. As long as the disruption process was able to break the cell walls and release the neutral lipid globules (without inflicting noticeable lipid degradation) for solvent solubilisation, the specific mechanism by which the wall breakage was achieved (e.g. shear by HPH or linkage hydrolysis by pH12) did not seem to contribute to the resulting neutral lipid mass transfer from the biomass into the solvent phase. Within the limits of our experiments, the HPH combinations generally achieved a higher cell disruption and thus a higher neutral lipid yield compared to pH12 combinations. For this reason, they occupied the upper half of the correlation in Fig. 4a.

Fig. 5 depicts our proposed mass-transfer mechanism for the extraction of neutral lipids from *Nannochloropsis* slurry using hexane. At partial cell disruption (i.e., extent of cell rupture $<$ 100% of cells in the slurry), a mixture of intact cells and disrupted cells exists in the slurry. When subjected to extraction with hexane, liberated lipid globules from the disrupted cells can interact with the solvent and diffuse out of the biomass, while those in the intact cells remain inaccessible to the solvent. Upon centrifugation, the solubilised lipids will partition in the hexane phase while those in the intact cells remain in the biomass. The lipid extraction efficiency is therefore proportional to the level of disrupted cells in the slurry. At complete cell disruption (i.e., extent of cell

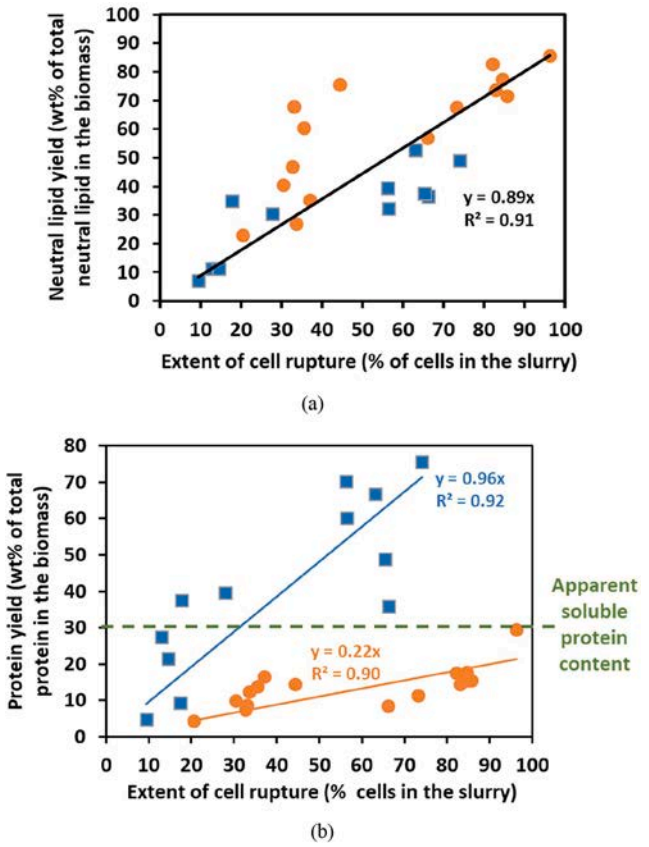

Fig. 4. (a) Correlation between neutral lipid yield and extent of cell rupture. (b) Correlations between protein yield and extent of cell rupture. ● mechanically disrupted biomass (HPH), ■ chemically disrupted biomass (pH 12). Results from all experimental replicates in Table 1 (exp 2,5,8, 11 for HPH; exp 3,6,9,12 for pH12) were collated to produce the correlations.

rupture 100% of cells in the slurry), all available cells in the slurry have been disrupted, leading to the release of all neutral lipid globules from cell-wall encapsulation. Hexane extraction of the slurry would therefore theoretically lead to complete solubilisation (and thus recovery) of all neutral lipids from the biomass. In practice, however, a level of residual neutral lipids would likely remain in the biomass due to incomplete solvent separation (i.e., the formation of post-centrifugation emulsion layer in Fig. 3a where some solvents containing dissolved lipids appeared to have partitioned together with the biomass in the aqueous phase). The proposed mass-transfer was valid across both mechanical (HPH) and chemical (pH12) disruption.

In terms of lipid compositions, no significant variations were found in the fatty acid profiles of neutral lipid extracts from different treatment combinations in Table 1. The fatty acids of neutral lipid extracts were comprised of the followings (in descending order): C16:1 (43.9 – 47.5 wt % of fatty acids), C16:0 (31.9 – 32.6 wt% of fatty acids), C18:1 (7.6 – 9.3 wt% of fatty acids), C20:5 (ω-3) (5.5 – 5.7 wt% of fatty acids), C14:0 (1.7 – 3.1 wt% of fatty acids), C20:3 (ω-6) (2.6 – 2.7 wt% of fatty acids) and C18:0 (1.4 – 1.5 wt% of fatty acids). The lack of variations in fatty acid profiles between the different treatment combinations can be attributed to the fact that identical neutral lipid extraction procedure deploying the same extraction solvent (hexane) under the same parameters (room temperature, slurry:hexane ratio 1:1 m/m) were used across all experiments throughout the study. Hexane is highly selective to neutral lipids and will only extract this fraction of the liberated lipids. Even though different pre-treatment and cell disruption combinations might render lipid fractions other than neutral lipid globules more accessible (e.g.,.glycolipids and phospholipids by pH12 hydrolysis), hexane would only recover the neutral lipid fractions that have been released from the biomass during cell disruption. These findings are in agreement with studies which showed that the fatty acid profiles of extracted microalgae lipids are more strongly determined by extraction solvents rather than biomass treatments (Mitra & Mishra, 2019; Ryckebosch et al., 2014).

3.5. *Relationship between cell disruption and protein recovery*

The pattern for protein extraction yield in Fig. 2c appeared to be in

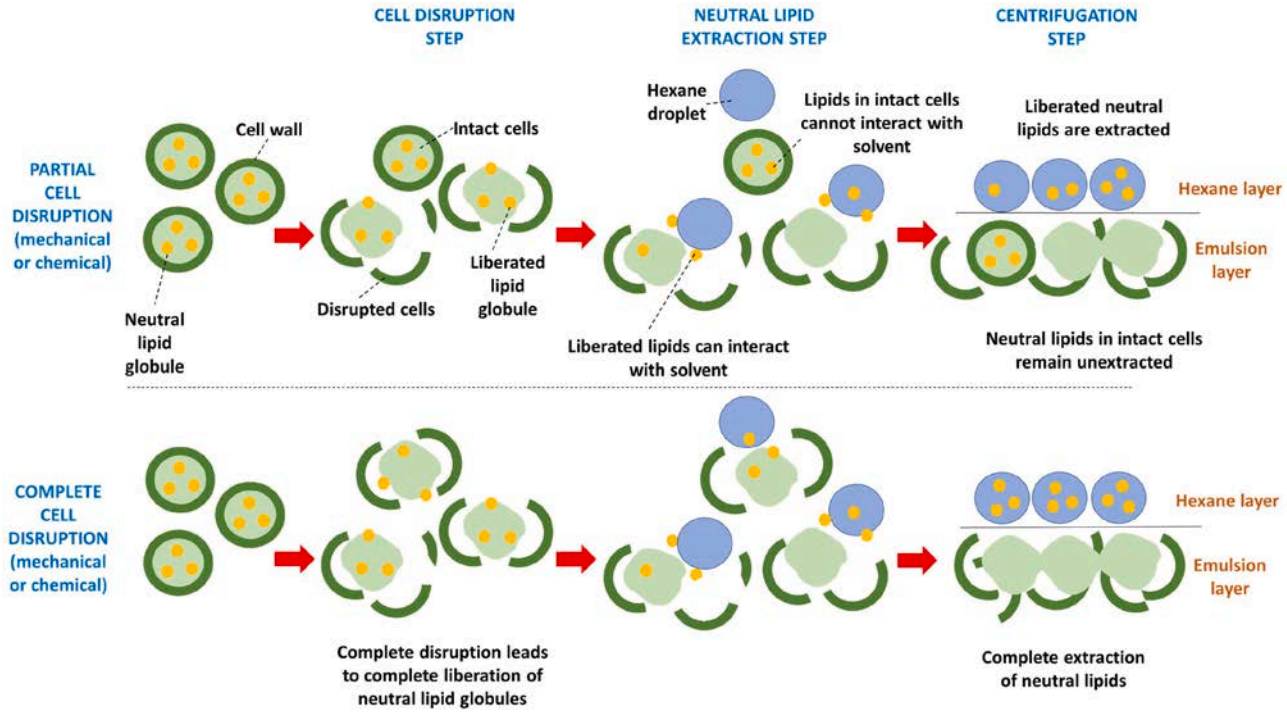

Fig. 5. Proposed mechanisms of neutral lipid extraction illustrating the direct dependence of neutral lipid yield on the extent of cell rupture.

opposite direction to the extent of cell rupture. The apparent protein yields of pH12 combinations were higher than those reported by HPH combinations, despite the chemical treatment's lower disruption efficiency. These results contradicted our initial understanding of the effect of cell disruption on product yield and prompted us to further probe the relationship between the two variables by plotting protein yield as a function of cell disruption across all HPH experiments and all pH12 experiments (Fig. 4b).

A plot of protein yield as a function of the extent of cell rupture generated two separate correlations, one for HPH combinations (or. mechanical treatment) and another for pH12 combinations (or chemical treatment). Unlike neutral lipid extraction, the behaviour of protein mass transfer was hence found to be dependent on the mode of cell disruption.

Both correlations established a positive relationship between protein yields and the extent of cell rupture, confirming that physical cell disintegration led to a higher protein release from the biomass into the interstitial space. However, the extent to which this release occurred was vastly different between pH12 experiments and HPH experiments. With a much steeper gradient (k 0.96), pH12 treatment was shown to be superior in facilitating protein release compared to HPH treatment (k 0.22). The discrepancy in extraction behaviours can be attributed to the complex nature of intracellular proteins and the differing abilities of the two disruption modes in interacting with different proteins.

Intracellular proteins exist as both non-structural proteins dissolved/suspended in the cytosols and structural proteins that form an integral component of the cell wall/membrane through biochemical linkages. Both types of proteins are 'trapped' by the cell walls. However, unlike non-structural proteins that can be 'freed' or liberated from the biomass by mere physical destruction of the cell walls, structural proteins require additional reactions able to severe their connection with cellular structure to be released (Phusunti & Cheirsilp, 2020; Safi et al., 2014; Scherer et al., 2019; Soto-Sierra et al., 2018). Without breaking the bonds that connect them to cell membranes/walls, structural proteins cannot be separated from the broken cell debris after cell disruption and simply partition in the biomass layer (instead of the aqueous layer, Fig. 3c,d) after centrifugation.

HPH disintegrated the cell walls through brute shear force mediated by physical collisions. Even though these actions were able to 'free' cytosolic proteins from the biomass, they failed to cleave structural proteins from the biomass. Mechanical disruption was therefore able to efficiently release cytosolic proteins, yet it had a limited capacity in liberating structural proteins. A closer inspection of the HPH curve verified this hypothesis. The curve had a positive gradient (albeit at a low value), demonstrating increased release of cytosolic proteins with cell rupture. However, the HPH curve had an imposed upper limit in the total amount of recoverable proteins. Despite being very effective in disintegrating cellular structure (i.e. the extent of cell rupture reaching almost 100% of cells for some experiments), the most efficient HPH combinations were only able to recover a maximum protein yield of 30%. This upper threshold in the level of extractable protein by HPH disruption represented the amount of cytosolic proteins available in the biomass. The structural proteins remained embedded in the cell debris after cell disruption (Safi et al., 2013).

Alkaline (pH12) treatment hydrolysed cell wall linkages and achieved cell disruption through slow solubilisation of cell-wall layers (Mendez et al., 2013; Safi et al., 2014; Wu et al., 2017). Chemical treatment is often carried out at extreme and highly degradative temperature range (greater than100℃) to exert sufficient disruption of thickly walled microalgae species (e.g. *Chlorella* sp. and *Nannochloropsis* sp) in slurry form (Laurens et al., 2015). However, the inclusion of pre-treatment steps in these experiments has considerably weakened the biomass to allow for significant disruption at mild conditions (T 65℃). Alkaline treatment had the capacity to achieve quantitative protein extraction as it was able to release both cytosolic proteins through cell wall disintegration and structural proteins through bond-cleaving reactions. A closer inspection of the pH12 curve in Fig. 4b confirmed this hypothesis. With a gradient close to one, the treatment can be projected to recover all available biomass proteins at 100% disruption efficiency (likely achievable by extending the duration of the alkali treatment or increasing pH).

Fig. 6 illustrates our proposed mass-transfer mechanisms for the extraction of proteins from *Nannochloropsis* slurry with either mechanical disruption or chemical disruption. For mechanical disruption, at partial cell disruption (i.e., extent of cell rupture $<$ 100% of cells in the slurry), a mixture of intact cells and disrupted cells exists in the slurry. Mechanical disruption's limited capacity in cleaving structural proteins means that only cytosolic proteins are released from the disrupted cells, while structural proteins in the cell fragments and all proteins in the intact cells remain inaccessible. Upon centrifugation, the water-soluble proteins will partition in the water phase while the structural proteins that remain attached to cell debris and proteins in the intact cells will partition in the cell-debris layer. At complete cell disruption (i.e., extent of cell rupture 100% of cells in the slurry), all available soluble proteins will be released (roughly 30% of all proteins in our biomass), while structural proteins will partition in the cell-debris layer and remain unextracted.

For chemical disruption, while the intracellular proteins in the intact cells remain inaccessible, the dual disruption mechanism catalysed by chemical hydrolysis will facilitate the release of both cytosolic and structural proteins from the ruptured cells. At partial disruption, an increase in the degree of cell rupture leads to more prolific release of intracellular proteins, establishing a proportional relationship between protein yields and the degree of cell rupture. Once separated, all available proteins from the ruptured cells will partition in the water phase, while proteins in the intact cells will remain in the biomass and partition in the cell-debris phase. At complete cell disruption, chemical disruption is able to release all available intracellular proteins, leading to the complete recovery of proteins from the biomass.

3.6. Perspective

The significance of the study is two-folds: Firstly, the study demonstrated of the use of novel biomass pre-treatments (i.e., autolytic incubation, hypotonic osmotic shock and the combination of the two methods) as robust platform technologies capable of significantly boosting the performance of biorefinery fractionation of concentrated *Nannochloropsis* slurries. In section 3.2, the pre-treatments were found to improve the efficiency of mechanical and chemical cell disruption of *Nannochloropsis* slurries by 1.4 – 4.9 folds. Both pre-treatments did not require the addition of chemicals and were non-degradative. Since both pre-treatments did not require the deployment of complex unit operations, they have minimum CAPEX and OPEX. Their integration into biorefineries can enhance the performance of subsequent cell disruption and potentially increase process efficiency through either increased product yields or reduction of processing cost as milder cell disruption steps are deployed.

The high cost of biomass processing remains a significant barrier to microalgae commercialisation, estimated to account between 20 and 60 % of overall production costs of microalgae products (Du et al., 2021; Mallick et al., 2016; Ruiz et al., 2016). Biomass drying is prohibitively energy intensive and can contribute up to 30% of the overall production cost (Du et al., 2021, Mallick et al., 2016). To minimise processing costs, it is critical to develop a biorefinery system able to process concentrated slurries, thus avoiding drying step altogether while at the same time operating at reduced volume (compared to dilute suspensions). The efficiency of microalgae cell disruption and product extraction steps, however, declines significantly when processing concentrated slurries, especially for species with thick cell walls such as *Nannochloropsis*. The pre-treatments developed in this study improve the performance of slurry processing and represent a stride towards a more scalable microalgae biorefinery. The commercial reality of the pre-treatment

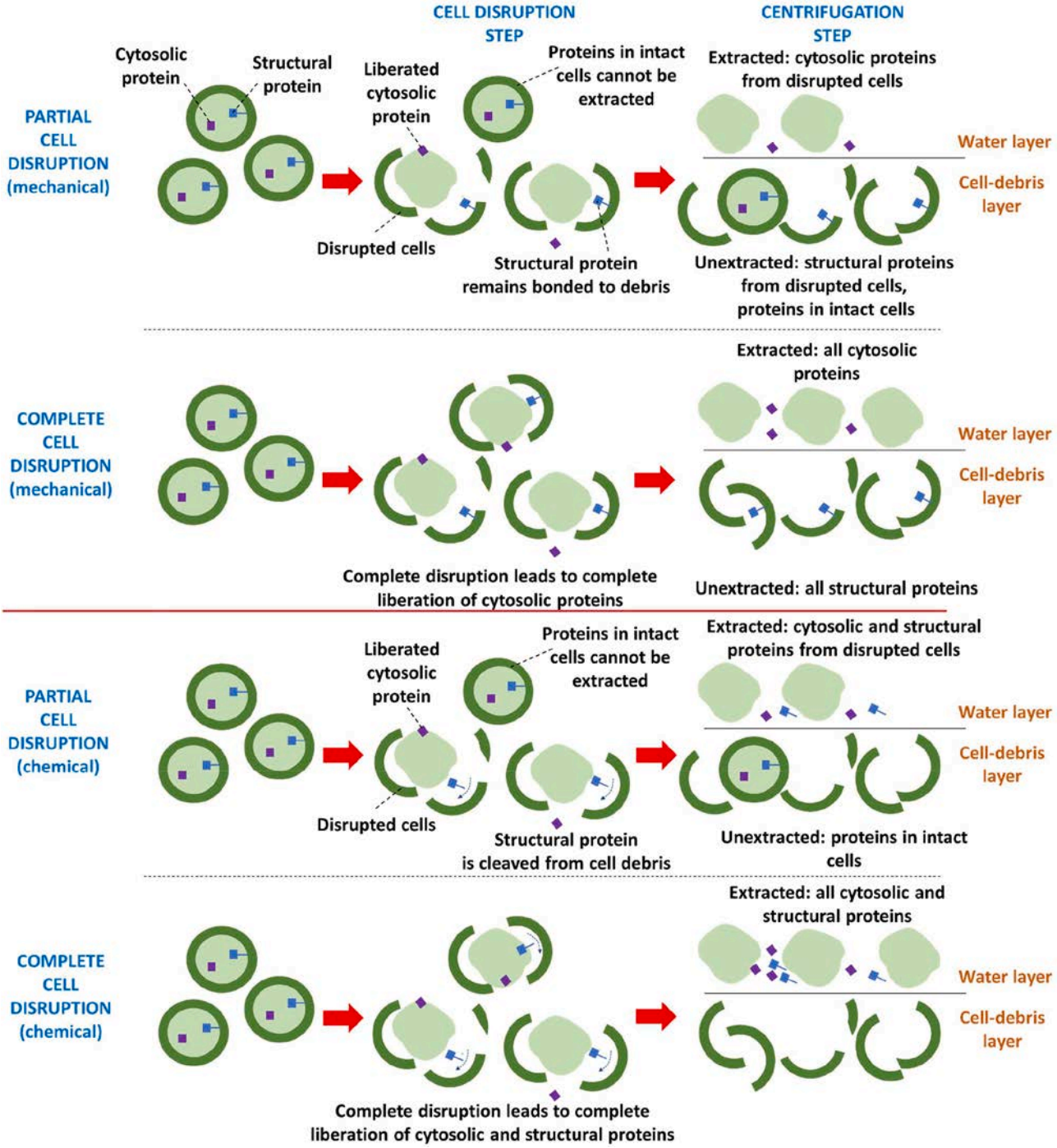

Fig. 6. Proposed mechanisms of protein extraction illustrating the complex dependence of protein recovery on both the extent of cell rupture and the hydrolysis of protein linkages.

steps, however, will require further scaling exercise and a case-by-case techno-economic assessment taking into consideration the specific target biorefinery and products. The transferability of the methods to other commercially promising microalgae genera beyond *Nannochloropsis* also warrants further investigation. When compared to other novel treatments recently reported in the literature (e.g., enzyme extracts isolated from filamentous fungi, hydrolysis using ruminal fluids, and enzyme + three-phase partitioning), the pre-treatments described in this study were found to be able to process slurries at much higher biomass concentration (see supplementary materials) (Alavijeh et al., 2020; Barragán-Trinidad et al., 2017; Monjed et al., 2020; Qiu et al., 2019; Sierra et al., 2017).

Secondly, through findings in section 3.4 and 3.5, the study provided novel insights into the mass-transfer behaviour of cytosolic and structural products from concentrated slurries. This will allow microalgae biorefinery operators to make more informed selection of their process specifications, potentially scaling down or reducing the intensity of ineffective disruption step and thus improving resource efficiency. For example, biorefineries aiming to generate products derived from cytosolic components (e.g., biodiesel) should aim for complete cell disruption using mechanical methods as this is requisite to achieve complete product recovery. On the other hand, biorefineries aiming to generate

products derived from structural components (e.g., protein) will require cell disruption that cleaves structural bonds instead of shear-based mechanical disruption that merely breaks cellular structure. For these biorefineries, the intensity of the cell disruption step can be minimised as complete disruption is not requisite for complete product recovery.

4. Conclusions

In conclusion, both autolytic incubation and hypotonic osmotic shock were highly effective in improving disruption efficiency (by 2.4–4.9 and 1.4–1.6 folds respectively). Neutral lipids exist as non-structural globules. Their release from the biomass was directly dependent on the degree of physical cell disruption. Shear-based HPH disruption was more effective in disrupting cells and resulted in higher yields. Intracellular proteins exist in both cytosolic and structural forms. Their release was dependent on both physical cell disruption and the severance of structural linkages. pH12 achieved cell disruption through the solubilisation of cell-wall/membrane linkages and released proteins more effectively compared to HPH.

CRediT authorship contribution statement

Ronald Halim: Conceptualization, Methodology, Validation, Formal analysis, Investigation, Funding acquisition. **Ioannis Papachristou:** Investigation. **George Q. Chen:** Formal analysis. **Huining Deng:** Formal analysis. **Wolfgang Frey:** Conceptualization, Resources. **Clemens Posten:** Conceptualization, Resources. **Aude Silve:** Conceptualization, Methodology, Resources, Project administration, Funding acquisition.

Declaration of Competing Interest

The authors declare that they have no known competing financial interests or personal relationships that could have appeared to influence the work reported in this paper.

Acknowledgements

RH is grateful for the generous supports received from the Alexander von Humboldt Postdoctoral Research Fellowship 2017 – 2018 (Ref 3.1-AUS-1192825-HFST-P). The authors would also like to thank the Helmholtz Research Program on Renewable Energies [Topic 3: Bioenergy] and EU's Horizon 2020 Research and Innovation program [Grant Agreement No. 727874] for their financial support.

References

Alavijeh, R.S., Karimi, K., Wijffels, R.H., van den Berg, C., Eppink, M., 2020. Combined bead milling and enzymatic hydrolysis for efficient fractionation of lipids, proteins, and carbohydrates of Chlorella vulgaris microalgae. Bioresour. Technol. 309, 123321.

Barragán-Trinidad, M., Carrillo-Reyes, J., Buitrón, G., 2017. Hydrolysis of microalgal biomass using ruminal microorganisms as a pretreatment to increase methane recovery. Bioresour. Technol. 244, 100–107.

Baudelet, P.-H., Ricochon, G., Linder, M., Muniglia, L., 2017. A new insight into cell walls of Chlorophyta. Algal Research 25, 333–371.

Bongiovani, N., Popovich, C.A., Martínez, A.M., Constenla, D., Leonardi, P.I., 2020. Biorefinery approach from nannochloropsis oceanica CCALA 978: neutral lipid and carotenoid co-production under nitrate or phosphate deprivation. Bioenergy Res. 13 (2), 518–529.

Canelli, G., Murciano Martínez, P., Austin, S., Ambühl, M.E., Dionisi, F., Bolten, C.J., Carpine, R., Neutsch, L., Mathys, A., 2021. Biochemical and morphological characterization of heterotrophic crypthecodinium cohnii and chlorella vulgaris cell walls. J. Agric. Food. Chem. 69 (7), 2226–2235.

Du, F., Wang, Y.-Z., Xu, Y.-S., Shi, T.-Q., Liu, W.-Z., Sun, X.-M., Huang, H., 2021. Biotechnological production of lipid and terpenoid from thraustochytrids. Biotechnol. Adv. 48, 107725.

Halim, R., 2020. Industrial extraction of microalgal pigments. Springer, Cham.

Halim, R., Danquah, M.K., Webley, P.A., 2012. Extraction of oil from microalgae for biodiesel production: A review. Biotechnol. Adv. 30 (3), 709–732.

Halim, R., Harun, R., Webley, P.A., Danquah, M.K., 2013. Bioprocess Engineering Aspects of Biodiesel and Bioethanol Production from Microalgae. In: Lee, J.W. (Ed.), Advanced Biofuels and Bioproducts. Springer, New York. New York, NY, pp. 601–628.

Halim, R., Hill, D.R.A., Hanssen, E., Webley, P.A., Blackburn, S., Grossman, A.R., Posten, C., Martin, G.J.O., 2019a. Towards sustainable microalgal biomass processing: anaerobic induction of autolytic cell-wall self-ingestion in lipid-rich Nannochloropsis slurries. Green Chem. 21 (11), 2967–2982.

Halim, R., Hill, D.R.A., Hanssen, E., Webley, P.A., Martin, G.J.O., 2019b. Thermally coupled dark-anoxia incubation: A platform technology to induce auto-fermentation and thus cell-wall thinning in both nitrogen-replete and nitrogen-deplete Nannochloropsis slurries. Bioresour. Technol. 290, 121769. https://doi.org/10.1016/j.biortech.2019.121769.

Halim, R., Papachristou, I., Kubisch, C., Nazarova, N., Wüstner, R., Steinbach, D., Chen, G.Q., Deng, H., Frey, W., Posten, C., Silve, A. 2020. Hypotonic osmotic shock treatment to enhance lipid and protein recoveries from concentrated saltwater Nannochloropsis slurries *Fuel*, **Accepted on 06/10/2020**.

Halim, R., Webley, P.A., Martin, G.J.O., 2016. The CIDES process: Fractionation of concentrated microalgal paste for co-production of biofuel, nutraceuticals, and high-grade protein feed. Algal Research 19, 299–306.

Hulatt, C.J., Wijffels, R.H., Bolla, S., Kiron, V., 2017. Production of Fatty Acids and Protein by Nannochloropsis in Flat-Plate Photobioreactors. PLoS ONE 12 (1), 1–17.

Jia, J., Han, D., Gerken, H.G., Li, Y., Sommerfeld, M., Hu, Q., Xu, J., 2015. Molecular mechanisms for photosynthetic carbon partitioning into storage neutral lipids in Nannochloropsis oceanica under nitrogen-depletion conditions. Algal Research 7, 66–77.

Laurens, L.M.L., Nagle, N., Davis, R., Sweeney, N., Van Wychen, S., Lowell, A., Pienkos, P.T., 2015. Acid-catalyzed algal biomass pretreatment for integrated lipid and carbohydrate-based biofuels production. Green Chem. 17 (2), 1145–1158.

Law, S.Q.K., Halim, R., Scales, P.J., Martin, G.J.O., 2018. Conversion and recovery of saponifiable lipids from microalgae using a nonpolar solvent via lipase-assisted extraction. Bioresour. Technol. 260, 338–347.

Lee, S.Y., Cho, J.M., Chang, Y.K., Oh, Y.-K., 2017. Cell disruption and lipid extraction for microalgal biorefineries: A review. Bioresour. Technol. 244, 1317–1328.

Li, T., Xu, J., Wu, H., Wang, G., Dai, S., Fan, J., He, H., Xiang, W., 2016. A saponification method for chlorophyll removal from microalgae biomass as oil feedstock. Mar. Drugs 14 (9), 162.

Mallick, N., Bagchi, S.K., Koley, S., Singh, A.K., 2016. Progress and challenges in microalgal biodiesel production. Front. Microbiol. 7 (1019).

Mendez, L., Mahdy, A., Timmers, R.A., Ballesteros, M., González-Fernández, C., 2013. Enhancing methane production of Chlorella vulgaris via thermochemical pretreatments. Bioresour. Technol. 149, 136–141.

Menegol, T., Romero-Villegas, G.I., López-Rodríguez, M., Navarro-López, E., López-Rosales, L., Chisti, Y., Cerón-García, M.C., Molina-Grima, E., 2019. Mixotrophic production of polyunsaturated fatty acids and carotenoids by the microalga Nannochloropsis gaditana. J. Appl. Phycol. 31 (5), 2823–2832.

Mitra, M., Mishra, S., 2019. A comparative analysis of different extraction solvent systems on the extractability of eicosapentaenoic acid from the marine eustigmatophyte Nannochloropsis oceanica. Algal Research 38, 101387. https://doi.org/10.1016/j.algal.2018.101387.

Monjed, M.K., Robson, G.D., Pittman, J.K., 2020. Isolation of fungal strains for biodegradation and saccharification of microalgal biomass. Biomass Bioenergy 137, 105547.

Olmstead, I.L.D., Hill, D.R.A., Dias, D.A., Jayasinghe, N.S., Callahan, D.L., Kentish, S.E., Scales, P.J., Martin, G.J.O., 2013. A quantitative analysis of microalgal lipids for optimization of biodiesel and omega-3 production. Biotechnol. Bioeng. 110 (8), 2096–2104.

Phusunti, N., Cheirsilp, B., 2020. Integrated protein extraction with bio-oil production for microalgal biorefinery. Algal Research 48, 101918.

Poddar, N., Sen, R., Martin, G.J.O., 2018. Glycerol and nitrate utilisation by marine microalgae Nannochloropsis salina and Chlorella sp. and associated bacteria during mixotrophic and heterotrophic growth. Algal Research 33, 298–309.

Qiu, C., He, Y., Huang, Z., Li, S., Huang, J., Wang, M., Chen, B., 2019. Lipid extraction from wet Nannochloropsis biomass via enzyme-assisted three phase partitioning. Bioresour. Technol. 284, 381–390.

Ruiz, J., Olivieri, G., de Vree, J., Bosma, R., Willems, P., Reith, J.H., Eppink, M.H.M., Kleinegris, D.M.M., Wijffels, R.H., Barbosa, M.J., 2016. Towards industrial products from microalgae. Energy Environ. Sci. 9 (10), 3036–3043.

Russo, G.L., Langellotti, A.L., Oliviero, M., Sacchi, R., Masi, P., 2021. Sustainable production of food grade omega-3 oil using aquatic protists: Reliability and future horizons. New Biotechnol. 62, 32–39.

Ryckebosch, E., Bruneel, C., Termote-Verhalle, R., Muylaert, K., Foubert, I., 2014. Influence of extraction solvent system on extractability of lipid components from different microalgae species. Algal Research 3, 36–43.

Safi, C., Cabas Rodriguez, L., Mulder, W.J., Engelen-Smit, N., Spekking, W., van den Broek, L.A.M., Olivieri, G., Sijtsma, L., 2017. Energy consumption and water-soluble protein release by cell wall disruption of Nannochloropsis gaditana. Bioresour. Technol. 239, 204–210.

Safi, C., Charton, M., Pignolet, O., Silvestre, F., Vaca-Garcia, C., Pontalier, P.-Y., 2013. Influence of microalgae cell wall characteristics on protein extractability and

determination of nitrogen-to-protein conversion factors. J. Appl. Phycol. 25 (2), 523–529.
Safi, C., Charton, M., Ursu, A.V., Laroche, C., Zebib, B., Pontalier, P.-Y., Vaca-Garcia, C., 2014. Release of hydro-soluble microalgal proteins using mechanical and chemical treatments. Algal Research 3, 55–60.
Safi, C., Olivieri, G., Engelen-Smit, N., Spekking, W., Veloo, R., den Broek, L.A.M.v., Sijtsma, L. 2020. Effect of growth conditions on the efficiency of cell disruption of Neochloris oleoabundans. *Bioresource Technology*, **300**, 122699.
Scherer, D., Krust, D., Frey, W., Mueller, G., Nick, P., Gusbeth, C., 2019. Pulsed electric field (PEF)-assisted protein recovery from Chlorella vulgaris is mediated by an enzymatic process after cell death. Algal Research 41, 101536.
Scholz, M.J., Weiss, T.L., Jinkerson, R.E., Jing, J., Roth, R., Goodenough, U., Posewitz, M.C., Gerken, H.G., 2014. Ultrastructure and composition of the nannochloropsis gaditana cell wall. Eukaryot. Cell 13 (11), 1450–1464.
Shene, C., Chisti, Y., Vergara, D., Burgos-Díaz, C., Rubilar, M., Bustamante, M., 2016. Production of eicosapentaenoic acid by Nannochloropsis oculata: effects of carbon dioxide and glycerol. J. Biotechnol. 239, 47–56.
Sierra, L.S., Dixon, C.K., Wilken, L.R., 2017. Enzymatic cell disruption of the microalgae Chlamydomonas reinhardtii for lipid and protein extraction. Algal Research 25, 149–159.
Simionato, D., Block, M.A., La Rocca, N., Jouhet, J., Maréchal, E., Finazzi, G., Morosinotto, T., 2013. The response of Nannochloropsis gaditana to nitrogen starvation includes de novo biosynthesis of triacylglycerols, a decrease of chloroplast galactolipids, and reorganization of the photosynthetic apparatus. Eukaryot Cell 12 (5), 665–676.
Simionato, D., Sforza, E., Corteggiani Carpinelli, E., Bertucco, A., Giacometti, G.M., Morosinotto, T., 2011. Acclimation of Nannochloropsis gaditana to different illumination regimes: Effects on lipids accumulation. Bioresour. Technol. 102 (10), 6026–6032.
Soto-Sierra, L., Stoykova, P., Nikolov, Z.L., 2018. Extraction and fractionation of microalgae-based protein products. Algal Research 36, 175–192.
Vanthoor-Koopmans, M., Wijffels, R.H., Barbosa, M.J., Eppink, M.H.M., 2013. Biorefinery of microalgae for food and fuel. Bioresour. Technol. 135, 142–149.
Wu, C., Xiao, Y., Lin, W., Li, J., Zhang, S., Zhu, J., Rong, J., 2017. Aqueous enzymatic process for cell wall degradation and lipid extraction from Nannochloropsis sp. Bioresour. Technol. 223, 312–316.
Yap, B.H.J., Crawford, S.A., Dagastine, R.R., Scales, P.J., Martin, G.J.O., 2016. Nitrogen deprivation of microalgae: effect on cell size, cell wall thickness, cell strength, and resistance to mechanical disruption. J. Ind. Microbiol. Biotechnol. 43 (12), 1671–1680.
Yap, B.H.J., Crawford, S.A., Dumsday, G.J., Scales, P.J., Martin, G.J.O., 2014. A mechanistic study of algal cell disruption and its effect on lipid recovery by solvent extraction. Algal Research 5, 112–120.